INSTITUTE OF PHYSICS PUBLISHING INVERSE PROBLEMS

Inverse Problems **22** (2006) 845–867 doi:10.1088/0266-5611/22/3/007

Analysis of two linear sampling methods applied to electromagnetic imaging of buried objects

Fioralba Cakoni[1], **M'Barek Fares**[2] **and Houssem Haddar**[3]

[1] Department of Mathematical Sciences, University of Delaware, Newark, DE 19716, USA
[2] CERFACS, 42 Avenue Coriolis, 31057 Toulouse Cedex 01, France
[3] INRIA Rocquencourt, BP 105, 78153, Le Chesnay Cedex, France

Received 28 August 2005, in final form 22 February 2006
Published 2 May 2006
Online at stacks.iop.org/IP/22/845

Abstract

We investigate two imaging methods to detect buried scatterers from electromagnetic measurements at a fixed frequency. The first one is the classical linear sampling method that requires the computation of Green's tensor for the background medium. This job can be numerically very costly for complex background geometries. The second one is an alternative approach based on the reciprocity gap functional that avoids the computation of Green's tensor but requires knowledge of both the electric and magnetic fields. Numerical examples are given showing the performance of both methods.

(Some figures in this article are in colour only in the electronic version)

1. Introduction

The inverse scattering problem of interest to us in this paper is that of determining the shape of a scattering object embedded in a known inhomogeneous medium from knowledge of the scattered electromagnetic field due to a point source incident field at a fixed frequency. We assume that the wavelength of the incident field has the same order of magnitude as the scatterer dimensions. The particular application we have in mind is the detection of objects buried in the earth from measurements of the total electromagnetic field on a given surface above the earth. The literature on this subject is particularly rich (e.g., [4, 19, 21] and the references therein), and for a scholarly review of some aspects of its history we refer the reader to [3]. Other potential applications may arise in medical imaging, nondestructive testing, etc.

Typically, in such applications, the physical properties of the scattering object are not known *a priori*. This is why the recently introduced imagining method, the so-called linear sampling method (LSM), known as being well adapted to this lack of information, can be of particular interest for these applications. For a scholarly review of this method we direct the reader to [9, 14, 18], while for applications of the linear sampling method to some basic inverse electromagnetic scattering problems we refer to [13, 24, 11]. This method is also known to be simple and relatively quick. However, when applied to inverse scattering problems for

buried objects its rapidity can be penalized by the cost of evaluating Green's function for the background medium [19, 21]. For a complex background medium, for instance, non-layered media, this evaluation can even be prohibitive. In a recent paper [12] by Colton and Haddar, a new version of the linear sampling method based on the *reciprocity gap functional* (RG-LSM) has been introduced which, in certain cases, avoids the need to compute Green's function for the background medium. To do so, it requires the existence of a bounded homogeneous region containing the scattering object and knowledge of the tangential components of both the total electric and magnetic fields on the boundary of this region. The RG-LSM also has the advantage of offering a more flexible mathematical framework than the classical linear sampling method: if the background medium is homogeneous, LSM is mathematically equivalent to a special case of RG-LSM [12]. It is also worth mentioning that the use of *reciprocity gap functional* here is different from what is classically done in solving other inverse problems (see [1, 4] for a review).

The aim of this paper is to validate theoretically and numerically the RG-LSM for solving the inverse electromagnetic scattering problems for buried objects in $\mathbb{R}^3$ and compare the performance of both the classical LSM and the RG-LSM. We remark that in our analysis of RG-LSM we remove the restrictive assumption in [12] on the location of the sources. To show the independence of this imaging method from the physical properties of the scatterer, we carry out the mathematical justification for two basic types of scatterers, namely perfect conductors and anisotropic penetrable objects. However, the numerical examples are restricted to the case of perfect conducting scatterers. The reason is only technical, since at the present time we do not have available a reliable forward code to produce synthetic data for a penetrable scatterer in an inhomogeneous background (see [24] for numerical examples in the case of inhomogeneous inclusions in a homogeneous background).

The plan of our paper is as follows. In the next section, we formulate the mathematical problems corresponding to the scattering of an electric dipole by a perfectly conducting obstacle as well as by an anisotropic inhomogeneity, both embedded in a known piecewise homogeneous background medium. We then proceed with an extended review of the linear sampling method for solving the inverse problem of determining the shape of the scattering object from knowledge of the tangential component of the electric field measured on a surface enclosing the scatterer. In section 4 we investigate the theory behind RG-LSM where only partial results are obtained. In particular, an open question remains whether the behaviour of the regularized numerical solution coincides with the behaviour of the predicted nearby solutions. We remark that substantial progress in this direction is made by Arens [2] for the LSM in the case of the Helmholtz equation. Having developed the analysis for the case of a perfect conductor, we prove the same results for the case of anisotropic inhomogeneities, where the analysis is more complex and relies on different mathematical tools. We also mention that the proof of lemma 4.6 given in this paper simplifies the arguments in the proof of the same result in [12]. We end the paper with a numerical validation of both sampling methods. In particular, we present numerical examples showing the viability of both imaging methods in the context of imaging buried perfect conductors in a two-layered medium. These first results are not representative of all the potentials of RG-LSM but only aim at validating this method in a simplified configuration. A more detailed numerical work, including, for instance, anisotropic inclusions and complex backgrounds is under preparation.

2. Formulation of the direct and inverse scattering problem

We consider the scattering of a time-harmonic electromagnetic field of frequency ω by a scattering object embedded in a piecewise homogeneous background in $\mathbb{R}^3$. We assume that

the magnetic permeability $\mu_0 > 0$ of the background medium is a positive constant whereas the electric permittivity $\epsilon(x)$ and conductivity $\sigma(x)$ are piecewise constant. Moreover, we assume that for $|x| = r > R$, for R sufficiently large, $\sigma = 0$ and $\epsilon(x) = \epsilon_0$. Then the electric field $\tilde{\mathcal{E}}$ and magnetic field $\tilde{\mathcal{H}}$ in the background medium satisfy the time-harmonic Maxwell's equations

$$\nabla \times \tilde{\mathcal{E}} - \mathrm{i}\omega\mu_0\tilde{\mathcal{H}} = 0, \qquad \nabla \times \tilde{\mathcal{H}} + (\mathrm{i}\omega\epsilon(x) - \sigma(x))\tilde{\mathcal{E}} = 0.$$

After an appropriate scaling [15] and elimination of the magnetic field, we now obtain the following equation for the electric field $\mathcal{E}$ in the background medium

$$\operatorname{curl}\operatorname{curl}\mathcal{E} - k^2 n(x)\mathcal{E} = 0,$$

where $\tilde{\mathcal{E}} = \frac{1}{\sqrt{\epsilon_0}}\mathcal{E}$, $k = \epsilon_0\mu_0\omega^2$ and $n(x) = \frac{1}{\epsilon_0}\big(\epsilon(x) + \mathrm{i}\frac{\sigma(x)}{\omega}\big)$. Note that the piecewise constant function $n(x)$ satisfies $n(x) = 1$ for $r > R$, $\operatorname{Re}(n) > 0$ and $\operatorname{Im}(n) \geqslant 0$. The surfaces across which $n(x)$ is discontinuous are assumed to be piecewise smooth and closed.

Now let D be a scattering object embedded in the above piecewise homogeneous background such that $\mathbb{R}^3\backslash\overline{D}$ is connected. We suppose that the boundary ∂D of D is piecewise smooth and denote by ν the outward unit normal. In this paper, we consider the cases when D is a perfect conductor or an inhomogeneous anisotropic penetrable object. Furthermore, we suppose that the incident field is an electric dipole located at $x_0 \in \Lambda$ with polarization $p \in \mathbb{R}^3$, where Λ is a smooth open surface situated in a layer with the constant index of refraction n_s, given by

$$E_e(x, x_0, p, k_s) := \frac{\mathrm{i}}{k_s}\operatorname{curl}_x\operatorname{curl}_x p\frac{\mathrm{e}^{\mathrm{i}k_s|x-x_0|}}{4\pi|x-x_0|} \tag{1}$$

where $k_s^2 = k^2 n_s$. We denote by $\mathbb{G}(x, x_0)$ the free space Green's tensor of the background medium and define $E^i(x) := E^i(x, x_0, p) = \mathbb{G}(x, x_0)p$ which satisfies

$$\operatorname{curl}\operatorname{curl}E^i(x) - k^2 n(x)E^i(x) = p\delta(x - x_0) \quad \text{in } \mathbb{R}^3, \tag{2}$$

where δ denotes the Dirac distribution. Note that E^i can be written as

$$E^i(x) = E_e(x, x_0, p, k_s) + E_b^s(x) \tag{3}$$

where $E_b^s = E_b^s(\cdot, x_0, p)$ is the electric scattered field due to the background medium.

In order to formulate precisely the scattering problem we recall the following Sobolev spaces. For a generic domain $\mathcal{O}$ with piecewise smooth boundary $\partial\mathcal{O}$ we define

$$\begin{aligned}
&H(\operatorname{curl}, \mathcal{O}) := \{u \in (L^2(\mathcal{O}))^3 : \nabla \times u \in (L^2(\mathcal{O}))^3\}\\
&L_t^2(\partial\mathcal{O}) := \{u \in (L^2(\partial\mathcal{O})^3 : \nu \cdot u = 0 \quad \text{on} \quad \partial\mathcal{O}\}\\
&L_{\operatorname{div}}^2(\partial\mathcal{O}) := \{u \in L_t^2(\partial\mathcal{O}) : \operatorname{div}_{\partial\mathcal{O}}u \in L^2(\partial\mathcal{O})\}.
\end{aligned}$$

where ν denotes the exterior normal to $\partial\mathcal{O}$ and $\operatorname{div}_{\partial\mathcal{O}}$ denotes the surface divergence. If $\mathcal{O}$ is unbounded we denote by $H_{\mathrm{loc}}(\operatorname{curl}, \mathcal{O})$ the space of functions $u \in H(\operatorname{curl}, K)$ for all compact sets $K \subset \mathcal{O}$. The traces $\nu \times u|_{\partial\mathcal{O}}$ and $\nu \times (u \times \nu)|_{\partial\mathcal{O}}$ of $u \in H(\operatorname{curl}, \mathcal{O})$ (or $u \in H_{\mathrm{loc}}(\operatorname{curl}, \mathcal{O})$) are in the following Hilbert spaces,

$$\begin{aligned}
H_{\operatorname{div}}^{-\frac{1}{2}}(\partial\mathcal{O}) &:= \big\{u \in \big(H^{-\frac{1}{2}}(\partial\mathcal{O})\big)^3, \quad \nu \cdot u = 0, \quad \operatorname{div}_{\partial\mathcal{O}}u \in H^{-\frac{1}{2}}(\partial\mathcal{O})\big\}\\
H_{\operatorname{curl}}^{-\frac{1}{2}}(\partial\mathcal{O}) &:= \big\{u \in \big(H^{-\frac{1}{2}}(\partial\mathcal{O})\big)^3, \quad \nu \cdot u = 0, \quad \operatorname{curl}_{\partial\mathcal{O}}u \in H^{-\frac{1}{2}}(\partial\mathcal{O})\big\}
\end{aligned}$$

respectively, with $\operatorname{curl}_{\partial\mathcal{O}}$ denoting the surface curl. Note that by an integration by parts we can define a duality relation between $H_{\operatorname{div}}^{-\frac{1}{2}}(\partial\mathcal{O})$ and $H_{\operatorname{curl}}^{-\frac{1}{2}}(\partial\mathcal{O})$ (see [29] in the case when the boundary is smooth, and [5, 6] in the case when the boundary is piecewise smooth).

We first assume that the scattering object is a perfect conductor. In this case the scattering problems is as follows:

Scattering by a perfect conductor. Given $E^i = E^i(\cdot, x_0, p) = \mathbb{G}(\cdot, x_0)p$, find a solution $E \in H_{\rm loc}(\text{curl}, \mathbb{R}^3\backslash\overline{D} \cup \{x_0\})$ of

$$\text{curl curl } E - k^2 n(x) E = 0 \quad \text{in } \mathbb{R}^3\backslash\overline{D} \cup \{x_0\}, \tag{4}$$

$$\nu \times E = 0 \quad \text{on } \partial D, \tag{5}$$

$$E^s := (E - E^i) \in H_{\rm loc}(\text{curl}, \mathbb{R}^3\backslash\overline{D}), \tag{6}$$

$$\lim_{r\to\infty} (\text{curl } E^s \times x - \text{ik}r E^s) = 0. \tag{7}$$

We refer to (4)–(7) as the problem (SPC). We remark that (4) is satisfied in the sense of distributions which implies the continuity of tangential components of E and curl E across the piecewise continuous interface where the index of refraction $n(x)$ changes [28].

Next we assume that D is an anisotropic penetrable scatterer having the same magnetic permeability μ_0 as the background medium. Again, after an appropriate scaling [15], the index of refraction of the scatterer is represented by a symmetric matrix-valued function denoted by $N(x)$, $x \in \overline{D}$, whose entries are bounded complex-valued functions such that $\bar{\xi} \cdot \text{Im}(N)\xi \geqslant 0$ and $\bar{\xi} \cdot \text{Re}(N)\xi \geqslant \gamma|\xi|^2$ for all $\xi \in \mathbb{C}^3$ and all $x \in \overline{D}$ where γ is a positive constant. We extend N to a 3×3 matrix defined in $\mathbb{R}^3$, denoted again by N, such that $N(x) = n(x)I$ for $x \in \mathbb{R}^3\backslash\overline{D}$, where $n(x)$ is the piecewise constant index of refraction of the background medium as described above. Then the scattering problem for an anisotropic medium is as follows:

Scattering by an anisotropic medium. Given $E^i = E^i(\cdot, x_0, p) = \mathbb{G}(\cdot, x_0)p$ satisfying (3), find a solution $E \in H_{\rm loc}(\text{curl}, \mathbb{R}^3\backslash\{x_0\})$ of

$$\text{curl curl } E - k^2 N(x) E = 0 \quad \text{in } \mathbb{R}^3\backslash\{x_0\}, \tag{8}$$

$$E^s := (E - E^i) \in H_{\rm loc}(\text{curl}, \mathbb{R}^3), \tag{9}$$

$$\lim_{r\to\infty} (\text{curl } E^s \times x - \text{ik}r E^s) = 0. \tag{10}$$

We refer to (8)–(10) as the problem (SIM). Here again (8) is satisfied in the sense of distributions which implies the continuity of tangential components of E and curl E across the interface where $N(x)$ has jumps [28].

The well-posedness of both problems (SPC) and (SIM) is well known (see, e.g., [25, 28]).

Remark 2.1. It is also possible to consider the problem of objects buried in an unbounded multilayer medium. In this case, the radiation condition and mathematical analysis of the forward become more complicated (see [20] for the case of a two-layered medium). However, the following analysis of the inverse scattering problems remains the same.

We now consider a bounded domain Ω such that $\overline{D}$ is contained in Ω and the open surface Λ is contained in $\mathbb{R}^3\backslash\overline{\Omega}$. Let Γ denote the piecewise smooth boundary of Ω. Note that Λ may be a subset of Γ. The *inverse scattering problem* we are interested in is to determine D from knowledge of the tangential components $\nu \times E$ and $\nu \times H$ of the total electric field $E = E(\cdot, x_0, p)$ and magnetic field $H = \frac{1}{\text{ik}}\text{curl } E$ measured on Γ for all point sources $x_0 \in \Lambda$ and two linearly independent polarizations p tangent to Λ at x_0. Here ν denotes the outward unit normal to Γ. We remark that in what follows ν is always the outward unit normal to the surface under consideration unless otherwise stated.

Adapting the proofs in [8, 26] to the case of near field data, one can prove that D is in fact uniquely determined from knowledge of the tangential components of the total electric and

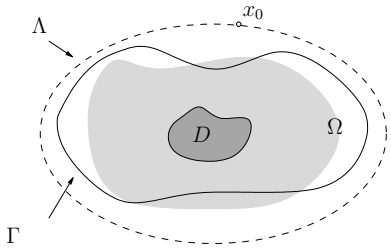

Figure 1. Example of a geometry for LSM.

magnetic field on Γ corresponding to all $x_0 \in \Lambda$ and two linearly independent polarizations p tangent to Λ at x_0. The main goal of this paper is the reconstruction of the shape of the scattering object D from the above-measured data by using the standard linear sampling method and a new version of the linear sampling method based on the reciprocity gap functional.

3. The linear sampling method: a review

In this section, we show how to use the linear sampling method to determine D from knowledge of the tangential component $\nu \times E(\cdot, x_0, p)|_\Gamma$ of the electric field only, for all $x_0 \in \Lambda$ and two linearly independent polarizations p tangent to Λ at x_0 (see figure 1). Note that for the linear sampling method the medium inside Ω does not need to be homogeneous.

Here we only sketch the main ideas of the method. For a scholarly review of the method, we refer the reader to [14, 18] and the references therein. The linear sampling method is based on finding a tangential field $\varphi_z \in L_t^2(\Lambda)$ that satisfies the following integral equation of the first kind referred to as the *near field equation*,

$$(\mathcal{F}\varphi_z)(x) := \int_\Lambda \nu(x) \times E^s(x, y, \varphi_z(y))\, \mathrm{d}s(y) = \nu(x) \times \mathbb{G}(x, z)q \tag{11}$$

for all $x \in \Gamma$, where $z \in \Omega$ and $q \in \mathbb{R}^3$ is an artificial polarization. Note that since E^s depends linearly on the polarization p, the *near field operator* $\mathcal{F} : L_t^2(\Lambda) \to L_t^2(\Gamma)$ is linear. We remind the reader that in our formulation of (SPC) and (SIM), E^s is the scattered field due to the incident wave being $E^i(x) = E_e(x, x_0, p, k_s) + E_b^s(x)$. Alternatively, one could replace E^s in the near field equation by the difference of the scattered field due to the point source $E_e(x, x_0, p, k_s)$ (which is in fact what we can physically measure) and the scattered field $E_b^s(x)$ due to the background medium.

By superposition $\mathcal{F}\varphi$ is the rotated tangential component on Γ of the scattered electric field corresponding to the potential

$$(\mathcal{S}\varphi)(x) := \int_\Lambda \varphi(y)\mathbb{G}(x, y)\, \mathrm{d}s(y) \tag{12}$$

as incident wave.

We first consider the case when the near field operator $\mathcal{F}$ corresponds to the scattering problem (SPC). From the uniqueness of the exterior boundary value problem with perfectly conducting boundary condition on Γ and the unique continuation principle, it is easy to show that for $z \in D$, φ_z is a solution to the near field equation (11) if and only if $\mathcal{S}\varphi_z$ solves the interior Maxwell problem

$$\operatorname{curl}\operatorname{curl} E - k^2 n(x) E = 0 \quad \text{in } D \tag{13}$$

$$\nu \times E = -\nu \times \mathbb{G}(\cdot, z)q \quad \text{on } \partial D. \tag{14}$$

Unfortunately, in general the solution to this problem is not a single layer potential. However, by similar arguments used in section 2 in [7] making use of approximation properties of potentials of the form (12), the unique continuation principle for the solutions to Maxwell's equations and the theory of ill-posed problems we can prove the following result (we remark that lemma 4.4 of this paper provides a proof for the approximation property of single layer potentials of a form slightly different from (12)). This proof can be easily carried out for potentials given by (12).

The values of k for which the homogeneous boundary value problem (13) and (14) with $\mathbb{G} = 0$ has a nontrivial solution are called *Maxwell eigenvalues* for D.

Theorem 3.1. *Assume that k is not a Maxwell eigenvalue for D and let $\mathcal{F}$ be the near field operator corresponding to (SPC). Then we have the following:*

(i) For $z \in D$ and a given $\epsilon > 0$, there exists a $\varphi_z^\epsilon \in L_t^2(\Lambda)$ such that

$$\left\| \mathcal{F}\varphi_z^\epsilon - \nu \times \mathbb{G}(\cdot, z)q \right\|_{L_t^2(\Gamma)} < \epsilon$$

and the corresponding potential $\mathcal{S}\varphi_z^\epsilon$ converges to the solution of (13) and (14) in $H(\text{curl}, D)$ as $\epsilon \to 0$.

(ii) For a fixed $\epsilon > 0$, we have that

$$\lim_{z \to \partial D} \left\| \mathcal{S}\varphi_z^\epsilon \right\|_{H(\text{curl}, D)} = \infty \qquad \text{and} \qquad \lim_{z \to \partial D} \left\| \varphi_z^\epsilon \right\|_{L_t^2(\Lambda)} = \infty.$$

(iii) For $z \in \mathbb{R}^3 \backslash \overline{D}$ and a given $\epsilon > 0$, every $\varphi_z^\epsilon \in L_t^2(\Lambda)$ that satisfies

$$\left\| \mathcal{F}\varphi_z^\epsilon - \nu \times \mathbb{G}(\cdot, z)q \right\|_{L_t^2(\Gamma)} < \epsilon$$

is such that

$$\lim_{\epsilon \to 0} \left\| \mathcal{S}\varphi_z^\epsilon \right\|_{H(\text{curl}, D)} = \infty \qquad \text{and} \qquad \lim_{\epsilon \to 0} \left\| \varphi_z^\epsilon \right\|_{L_t^2(\Lambda)} = \infty.$$

We next consider the case when the near field operator $\mathcal{F}$ corresponds to the scattering problem (SIM). Again, from the uniqueness of the exterior boundary value problem with the perfectly conducting boundary condition on Γ and the unique continuation principle, one can easily show that for $z \in D$, (11) has a solution if and only if the *interior transmission problem*

$$\text{curl curl } E_0 - k^2 n(x) E_0 = 0 \quad \text{in } D \tag{15}$$

$$\text{curl curl } E^{\text{int}} - k^2 N(x) E^{\text{int}} = 0 \quad \text{in } D \tag{16}$$

$$\nu \times E^{\text{int}} - \nu \times E_0 = \nu \times \mathbb{G}(\cdot, z)q \quad \text{on } \partial D \tag{17}$$

$$\nu \times \text{curl } E^{\text{int}} - \nu \times \text{curl } E_0 = \nu \times \text{curl } \mathbb{G}(\cdot, z)q \quad \text{on } \partial D \tag{18}$$

has a solution with $E_0 = \mathcal{S}\varphi_z|_D$. The values of k for which the homogeneous problem (15)–(18) with $\mathbb{G} = 0$ has a nontrivial solution are called *transmission eigenvalues*. The solvability of the interior transmission problem (15)–(18) in the case when $n(x) = 1$ is studied in detail in [23]. The analysis in [23] can be carried out in the case where $n(x) \neq 1$. Note that in the particular case when the domain Ω surrounding the scatterer D is homogeneous, we obtain exactly the problem studied in [23]. Based on the solvability result of the interior transmission problem, approximation properties of the potential (12), the unique continuation principle for the solutions to Maxwell's equations and the theory of ill-posed problems, by modifying the argument used in [10, 23] (see also [21] in the case of linear elasticity) we can prove the following result:

Theorem 3.2. *Assume that k is not a transmission eigenvalue and $(N - nI)$ is invertible. Let $\mathcal{F}$ be the near field operator corresponding to (SIM). Then*

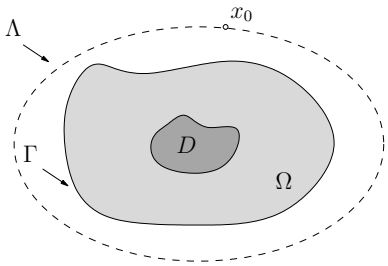

Figure 2. Example of a geometry for RG-LSM.

(i) For $z \in D$ and a given $\epsilon > 0$, there exists a $\varphi_z^\epsilon \in L_t^2(\Lambda)$ such that

$$\left\| \mathcal{F}\varphi_z^\epsilon - \nu \times \mathbb{G}(\cdot, z)q \right\|_{L_t^2(\Gamma)} < \epsilon$$

and the corresponding potential $\mathcal{S}\varphi_z^\epsilon$ converges to a function E_0 in $H(\text{curl}, D)$ as $\epsilon \to 0$, where (E_0, E) is the solution of the interior transmission problem (15)–(18).

Parts (ii) and (iii) of theorem 3.1 are also valid in this case.

Theorems 3.1 and 3.2 provide a characterization of the boundary ∂D of the scattering object D. Unfortunately, since the behaviour of $\mathcal{S}\varphi_z^\epsilon$ is described in terms of a norm depending on the unknown region D, $\mathcal{S}\varphi_z^\epsilon$ cannot be used to characterize D. Instead the linear sampling method characterizes the obstacle by the behaviour of φ_z^ϵ. In particular, given a discrepancy $\epsilon > 0$ and φ_z^ϵ the ϵ-approximate solution of the near field equation, the boundary of the scatterer is reconstructed as the set of points z where the $L_t^2(\Lambda)$ norm of φ_z^ϵ becomes large. The numerical implementation of the linear sampling method is discussed in section 4.

In practice, since the near field equation is severely ill-posed due to the compactness of the operator $\mathcal{F}$, one uses regularization methods to obtain a solution to (11). Obviously, an important question is whether this regularized solution will exhibit the properties of the ϵ-approximate solution provided by theorems 3.1 and 3.2. In general, this question is still open. Progress towards the answer of the above question is recently made by Arens in [2] in the case of the scalar problem for a perfect conductor in a homogeneous background using far field data. In particular, it is shown that the regularized solution obtained by standard regularization strategies behaves as the theoretical analysis predicts. Numerical examples also confirm that this is indeed the case [11, 13, 22, 24].

Even though the linear sampling method, in principle, can be used in the case of a quite general inhomogeneous background, the main drawback of the method in this case is the need to compute the background Green's function. In the next section we show how, at the expense of additional data and restrictions, one can avoid the need to compute the background Green's function.

4. The reciprocity gap functional

We need to make two additional assumptions. First, we assume that the medium inside the domain Ω containing the scattering object D is homogeneous with the constant index of refraction n_b and define $k_b^2 = k^2 n_b$ (see figure 2).

Second, we assume that *both* the tangential components $\nu \times E$ and $\nu \times H$ of the total electric field $E = E(\cdot, x_0, p)$ and magnetic field $H = \frac{1}{ik}\text{curl}\, E$, respectively, are known on Γ for all point sources $x_0 \in \Lambda$. In other words, we assume that we know $\nu \times E|_\Gamma$ and $\nu \times \text{curl}\, E|_\Gamma$

for all $x_0 \in \Lambda$. Furthermore, without loss of generality, we assume that Λ is a closed surface surrounding Ω situated in a layer with the index of refraction n_s. By an analyticity argument, the following analysis also holds true if the point sources are located on an open analytic surface provided it can be extended to a closed (analytic) surface as above.

Hence, for any function $W \in H(\text{curl}, \Omega)$, we can define the *gap reciprocity functional* by

$$\mathcal{R}(E, W) = \int_\Gamma (\nu \times E) \cdot \text{curl}\, W - (\nu \times W) \cdot \text{curl}\, E \, \text{d}s. \tag{19}$$

Since $E \in H(\text{curl}, \Omega)$, the integral is interpreted in the sense of the duality between $H_{\text{div}}^{-\frac{1}{2}}(\Gamma)$ and $H_{\text{curl}}^{-\frac{1}{2}}(\Gamma)$. Note that E depends on x_0 and hence so does $\mathcal{R}$. Next we define the subspace $\mathbb{H}(\Omega) \subset H(\text{curl}, \Omega)$ by

$$\mathbb{H}(\Omega) := \left\{ W \in H(\text{curl}, \Omega) : \text{curl}\,\text{curl}\, W - k_b^2 W = 0 \right\}.$$

The reciprocity gap functional restricted to $\mathbb{H}(\Omega)$ can be seen as an operator $R : \mathbb{H}(\Omega) \to L_t^2(\Lambda)$ defined by

$$R(W)(x_0) \cdot p(x_0) = \mathcal{R}(E(\cdot, x_0, p(x_0)), W) \tag{20}$$

for all $x_0 \in \Lambda$ and $p(x_0)$ a tangent vector to Λ at x_0.

In order to set up a solvable equation in terms of $\mathcal{R}$, we need to use a parametric family of solutions in $\mathbb{H}(\Omega)$ which satisfies certain properties to be made precise later. In particular, we define the electric Herglotz function $\mathcal{H}g$ by

$$\mathcal{H}g(x) := \int_{S^2} g(d)\, \text{e}^{\text{i}k_b d \cdot x} \, \text{d}s(d), \qquad g \in L_t^2(S^2) \tag{21}$$

where S^2 is the unit sphere and the single layer potential $A\varphi$ is given by

$$(A\varphi)(x) := \text{curl}\,\text{curl} \int_{\tilde{\Lambda}} \varphi(y) \Phi(x, y, k_b) \, \text{d}s, \qquad \varphi \in L_{\text{div}}^2(\tilde{\Lambda}) \tag{22}$$

where

$$\Phi(x, y, k_b) := \frac{1}{4\pi} \frac{\text{e}^{\text{i}k_b|x-y|}}{|x-y|}, \qquad x \neq y,$$

and $\tilde{\Lambda}$ is a regular part of the boundary of some simply connected domain containing Ω in its interior. Now, letting

$$E_e(x, z, q, k_b) = \frac{\text{i}}{k} \text{curl}_x\, \text{curl}_x q \Phi(x, z, k_b), \qquad q \in \mathbb{R}^3 \tag{23}$$

denote the electric dipole corresponding to k_b, we look for a solution $g \in L_t^2(S^2)$ to

$$\mathcal{R}(E, \mathcal{H}g) = \mathcal{R}(E, E_e(\cdot, z, q, k_b)) \tag{24}$$

or a solution $\varphi \in L_{\text{div}}^2(\tilde{\Lambda})$ of

$$\mathcal{R}(E, A\varphi) = \mathcal{R}(E, E_e(\cdot, z, q, k_b)). \tag{25}$$

Note that both $\left\{ \mathcal{H}g, g \in L_t^2(S^2) \right\}$ and $\left\{ A\varphi, \varphi \in L_{\text{div}}^2(\tilde{\Lambda}) \right\}$ are subsets of $\mathbb{H}(\Omega)$. The reciprocity gap functional method is based on the characterization of D from the behaviour of g or φ for different sampling points $z \in \Omega$. This method is in fact a new version of the linear sampling method since it provides an indicator function whose behaviour depends on the location of the sampling point z with respect to D and this indicator function is a solution to a linear integral equation. In particular, by similar calculations as in [12], we can show that if the background medium is homogeneous, the incident field is a plane wave and the far field pattern is used as the given data, then (24) becomes the far field equation which is used in the linear sampling method.

4.1. The reciprocity gap functional for a perfect conductor

Let $E = E(\cdot, x_0, p) = E^s(\cdot, x_0, p) + \mathbb{G}(\cdot, x_0)p$ and $H = 1/ik\operatorname{curl} E$ be the total electric and magnetic fields, respectively, corresponding to the scattering problem (SPC). Note that we suppress the dependence of the total field on the wave number k_s of the medium where the point source is located.

Lemma 4.1. *Assume that k_b is not a Maxwell eigenvalue for D. Then the operator $R : \mathbb{H}(\Omega) \to L_t^2(\Lambda)$ defined by (20) is injective.*

Proof. $RW = 0$ means $\mathcal{R}(E(\cdot, x_0, p(x_0)), W) = 0$ for all $(x_0, p(x_0))$ as in (20). Since both E and W satisfy Maxwell's equation in $\Omega\backslash\overline{D}$, we have, using the boundary condition on ∂D,

$$0 = \int_\Gamma (\nu \times E) \cdot \operatorname{curl} W - (\nu \times W) \cdot \operatorname{curl} E \, \mathrm{d}s = -\int_{\partial D} (\nu \times W) \cdot \operatorname{curl} E \, \mathrm{d}s.$$

It suffices to show that the set $L := \{(\operatorname{curl} E(\cdot, x_0, p(x_0)))_\top : x_0 \in \Lambda\}$ is dense in $H_{\operatorname{curl}}^{-\frac{1}{2}}(\partial D)$. Indeed, this fact implies that $\nu \times W = 0$ on ∂D and from the uniqueness of the solution to (13) and (14) we have that $W = 0$ in D, whence by the unique continuation principle we obtain $W = 0$ in Ω.

To prove the denseness property, let $f \in H_{\operatorname{div}}^{-\frac{1}{2}}(\partial D)$ and assume that

$$\int_{\partial D} f \cdot (\nu \times \operatorname{curl} E) \, \mathrm{d}s = 0$$

for all total fields E such that $(\operatorname{curl} E)_\top \in L$. Let $\tilde{E}$ be the unique solution to

$$\begin{aligned} &\operatorname{curl}\operatorname{curl} \tilde{E} - k^2 n(x) \tilde{E} = 0 \quad \text{in } \mathbb{R}^3\backslash\overline{D} \\ &\nu \times \tilde{E} = f \quad \text{on } \partial D \\ &\lim_{r\to\infty} (\operatorname{curl}\tilde{E} \times x - \mathrm{i}kr\tilde{E}) = 0. \end{aligned}$$

By a duality argument, we have that

$$\begin{aligned} 0 &= \int_{\partial D} f \cdot (\nu \times \operatorname{curl} E) \, \mathrm{d}s = \int_{\partial D} \tilde{E} \cdot [\nu \times \operatorname{curl}(E^s + \mathbb{G}(\cdot, x_0)p)] \, \mathrm{d}s \\ &= \int_{\partial D} \tilde{E} \cdot (\nu \times \operatorname{curl} E^s) \, \mathrm{d}s + \int_{\partial D} \tilde{E} \cdot (\nu \times \operatorname{curl} \mathbb{G}(\cdot, x_0)p) \, \mathrm{d}s. \end{aligned} \tag{26}$$

Since both E^s and $\tilde{E}$ are radiating solutions to $\operatorname{curl}\operatorname{curl} E - k^2 n(x) E = 0$ outside D, by applying the vector Green's formula we have that

$$\int_{\partial D} \tilde{E} \cdot (\nu \times \operatorname{curl} E^s) \, \mathrm{d}s = \int_{\partial D} E^s \cdot (\nu \times \operatorname{curl} \tilde{E}) \, \mathrm{d}s. \tag{27}$$

Substituting (27) into (26) and using the boundary condition $\nu \times E^s = -\nu \times \mathbb{G}(\cdot, x_0)p$ on ∂D we have that

$$0 = \int_{\partial D} \tilde{E} \cdot (\nu \times \operatorname{curl} \mathbb{G}(\cdot, x_0)p) \, \mathrm{d}s + \int_{\partial D} E^s \cdot (\nu \times \operatorname{curl} \tilde{E}) \, \mathrm{d}s = p \cdot \tilde{E}(x_0).$$

Since p is an arbitrary polarization in the tangent plane to Λ at x_0, we obtain $\nu \times \tilde{E}(x_0) = 0$ for $x_0 \in \Lambda$. Furthermore, since $\tilde{E}$ is a radiating solution to Maxwell's equations outside the domain bounded by Λ, we conclude by the uniqueness theorem for the scattering problem for a perfect conductor (cf [15]) that $\tilde{E} = 0$ outside the domain bounded by Λ. Then the unique continuation principle implies that $\tilde{E} = 0$ outside D, whence $f = 0$, which proves the lemma. □

Lemma 4.2. *Assume that k_b is not a Maxwell eigenvalue for D. Then the operator $R : \mathbb{H}(\Omega) \to L_t^2(\Lambda)$ defined by (20) has a dense range.*

Proof. Consider $\alpha \in L_t^2(\Lambda)$ and assume that

$$(RW, \alpha)_{L_t^2(\Lambda)} = 0 \text{ for all } W \in \mathbb{H}(\Omega).$$

From (20) and the bilinearity of $\mathcal{R}$ one has

$$(RW, \alpha)_{L_t^2(\Lambda)} = \int_\Lambda \mathcal{R}(E(\cdot, x_0, \alpha(x_0)), W)\, \mathrm{d}s(x_0) = \mathcal{R}(\mathcal{E}, W),$$

where

$$\mathcal{E}(x) = \int_\Lambda E(x, x_0, \alpha(x_0))\, \mathrm{d}s(x_0). \tag{28}$$

Using Green's vector formulae and the boundary condition on ∂D one concludes that

$$0 = \mathcal{R}(\mathcal{E}, W) = -\int_{\partial D} \operatorname{curl} \mathcal{E} \cdot (\nu \times W)\, \mathrm{d}s \tag{29}$$

for all $W \in \mathbb{H}(\Omega)$. Since $\mathbb{H}(\Omega)$ contains the Herglotz wavefunctions given by (21), from [16] one has that the set of $(\nu \times W)|_{\partial D}$ is dense in $H_{\mathrm{div}}^{-\frac{1}{2}}(\partial D)$. Therefore

$$\operatorname{curl} \mathcal{E} \times \nu = 0 \text{ on } \partial D.$$

Since $\mathcal{E} \times \nu = 0$ on ∂D as well, the extension of $\mathcal{E}$ by 0 inside D satisfies Maxwell's equations inside the domain bounded by Λ with the index n set equal to n_b inside D. From the unique continuation principle, one has that $\mathcal{E}$ is 0 inside the domain bounded by Λ and outside D. Noting that

$$\mathcal{E}(x) = \int_\Lambda (E^s(x, x_0, \alpha(x_0)) + \mathbb{G}(x, x_0)\alpha(x_0))\, \mathrm{d}s(x_0)$$

one concludes that $\mathcal{E} \times \nu$ is continuous across Λ. The uniqueness theorem of the exterior problem for Maxwell's equations with boundary data $\nu \times \mathcal{E} = 0$ on Λ implies that $\mathcal{E} = 0$ outside the domain bounded by Λ as well. Finally, from the jump relations of the vector potential across Λ [15] we have that

$$0 = \operatorname{curl} \mathcal{E}|_{\Lambda^+} - \operatorname{curl} \mathcal{E}|_{\Lambda^-} = -\alpha \quad \text{on } \Lambda$$

which ends the proof. □

We first investigate the solvability of

$$\mathcal{R}(E, \mathcal{H}g) = \mathcal{R}(E, E_e(\cdot, z, q, k_b)) \tag{30}$$

with respect to g where $E_e(\cdot, z, q, k_b)$ is given by (23) and $\mathcal{H}g$ is the electric Herglotz function with kernel g given by (21). To this end, we consider the interior boundary value problem

$$\operatorname{curl} \operatorname{curl} W - k^2 n_b W = 0 \quad \text{in } D \tag{31}$$

$$\nu \times W = E_e(\cdot, z, q, k_b) \quad \text{on } \partial D \tag{32}$$

which has a solution provided that k is not a Maxwell eigenvalue for D (i.e., k is not such that the homogeneous problem corresponding to (31) and (32) has nontrivial solution). The following result holds:

Theorem 4.3. *Assume that k is not a Maxwell eigenvalue for D and let $E = E(\cdot, x_0, p)$ and $H = 1/\mathrm{i}k \operatorname{curl} E$ be the total electric and magnetic fields, respectively, corresponding to the scattering problem (SPC). Then we have the following:*

(i) For $z \in D$ and a given $\epsilon > 0$, there exists a $g_z^\epsilon \in L_t^2(S^2)$ such that

$$\left\| \mathcal{R}\left(E, \mathcal{H}g_z^\epsilon\right) - \mathcal{R}(E, E_e(\cdot, z, q, k_b)) \right\|_{L_t^2(\Lambda)} < \epsilon$$

and the corresponding electric Herglotz wavefunction $\mathcal{H}g_z^\epsilon$ converges to the solution of (31) and (32) in $H(\text{curl}, D)$ as $\epsilon \to 0$.

(ii) For a fixed $\epsilon > 0$, we have that

$$\lim_{z \to \partial D} \left\| \mathcal{H}g_z^\epsilon \right\|_{H(\text{curl}, D)} = \infty \qquad \text{and} \qquad \lim_{z \to \partial D} \left\| g_z^\epsilon \right\|_{L_t^2(S^2)} = \infty.$$

(iii) For $z \in \mathbb{R}^3 \backslash \overline{D}$ and a given $\epsilon > 0$, every $g_z^\epsilon \in L_t^2(S^2)$ that satisfies

$$\left\| \mathcal{R}\left(E, \mathcal{H}g_z^\epsilon\right) - \mathcal{R}(E, E_e(\cdot, z, q, k_b)) \right\|_{L_t^2(\Lambda)} < \epsilon$$

is such that

$$\lim_{\epsilon \to 0} \left\| \mathcal{H}g_z^\epsilon \right\|_{H(\text{curl}, D)} = \infty \qquad \text{and} \qquad \lim_{\epsilon \to 0} \left\| g_z^\epsilon \right\|_{L_t^2(S^2)} = \infty.$$

Proof. Let $z \in D$. Since $W \in \mathbb{H}(\Omega)$ and $E_e(\cdot, z, q, k_b)$ satisfy $\text{curl}\,\text{curl}\, W - k_b W = 0$ in $\Omega \backslash \overline{D}$, integrating by parts and using the boundary condition for the total field we have that

$$\mathcal{R}(E, W) - \mathcal{R}(E, E_e(\cdot, z, q, k_b)) = -\int_{\partial D} (\nu \times W - \nu \times E_e(\cdot, z, q, k_b)) \cdot \text{curl}\, E \, \mathrm{d}s.$$

From the proof of lemma 4.1 we see that $\mathcal{R}(E, W) = \mathcal{R}(E, E_e(\cdot, z, q, k_b))$ has a unique solution W if and only if there exists a $W \in \mathbb{H}(\Omega)$ such that $\nu \times W = \nu \times E_e(\cdot, z, q, k_b) = 0$ on ∂D which is in general not true. However, in [16] it is proved that the family $\left\{\mathcal{H}g,\, g \in L_t^2(S^2)\right\}$ is dense in $H(\text{curl}, \Omega)$. Hence, from the trace theorem, for every $\epsilon > 0$ there exists a Herglotz function $\mathcal{H}g_z^\epsilon$ such that $\nu \times \mathcal{H}g_z^\epsilon$ approximates $\nu \times E_e(\cdot, z, q)$ with respect to the $H_{\text{div}}^{-\frac{1}{2}}(\partial D)$ norm. In particular, g_z^ϵ is an approximate solution to (30) and $\nu \times \mathcal{H}g_z^\epsilon$ converges to the solution of (31) and (32) in the $H(\text{curl}, D)$ norm as $\epsilon \to 0$. Next, since $\|\nu \times E_e(\cdot, z, q)\|_{H_{\text{div}}^{-\frac{1}{2}}(\partial D)}$ blows up as z approaches the boundary, we obtain that, for a fixed $\epsilon > 0$, $\lim_{z \to \partial D} \left\| \nu \times \mathcal{H}g_z^\epsilon \right\|_{H_{\text{div}}^{-\frac{1}{2}}(\partial D)} = \infty$ and consequently $\lim_{z \to \partial D} \left\| \mathcal{H}g_z^\epsilon \right\|_{H(\text{curl}, D)} = \infty$ and $\lim_{z \to \partial D} \left\| g_z^\epsilon \right\|_{L_t^2(S^2)} = \infty$.

Now we consider $z \in \Omega \backslash \overline{D}$ and let g_z^ϵ and its corresponding Herglotz function $\mathcal{H}g_z^\epsilon$ be such that

$$\left\| \mathcal{R}\left(E, \mathcal{H}g_z^\epsilon\right) - \mathcal{R}(E, E_e(\cdot, z, q, k_b)) \right\|_{L^2(\Lambda)} < \epsilon. \tag{33}$$

Note that from lemma 4.2 we can always find such a $\mathcal{H}g_z^\epsilon$. Assume to the contrary that $\left\| \mathcal{H}g_z^\epsilon \right\|_{H(\text{curl}, D)} < C$ where the positive constant C is independent of ϵ. From the trace theorem we have that $\nu \times \mathcal{H}g_z^\epsilon$ is also bounded in the $H_{\text{div}}^{-\frac{1}{2}}(\partial D)$ norm. Noting that the total field can be written as $E(\cdot, x_0, p) = E^s(\cdot, x_0, p) + \mathbb{G}(\cdot, x_0)p$ and integrating by parts, we obtain that

$$\begin{aligned}
\mathcal{R}(E, E_e(x, z, q, k_b)) = &\int_\Gamma (\nu \times E^s(x, x_0, p)) \cdot \text{curl}\, E_e(x, z, q, k_b) \, \mathrm{d}s_x \\
&- \int_\Gamma (\nu \times E_e(x, z, q, k_b)) \cdot \text{curl}\, E^s(x, x_0, p) \, \mathrm{d}s_x \\
&+ \int_\Gamma (\nu \times \mathbb{G}(x, x_0)p) \cdot \text{curl}\, E_e(x, z, q, k_b) \, \mathrm{d}s_x \\
&- \int_\Gamma (\nu \times E_e(x, z, q, k_b)) \cdot \text{curl}\, \mathbb{G}(x, x_0)p \, \mathrm{d}s_x.
\end{aligned}$$

Due to the symmetry of the background Green's function, $E^s(x, x_0, p)$ as a function of x_0 solves $\operatorname{curl}_{x_0}\operatorname{curl}_{x_0} E^s(x, x_0, p) - k^2 n(x_0) E^s(x, x_0, p) = 0$ in the domain bounded by Λ and ∂D. Hence the first two integrals in the above equation give a solution $W(x_0)$ to the same equation as $E^s(\cdot, x_0, p)$, while the last two integrals add up to $-\mathbb{G}(z, x_0)p$ by the Stratton–Chu formula and the fact that $E_e(x, z, q, k_b)$ is the fundamental solution of $\operatorname{curl}\operatorname{curl} E - k_b^2 E = 0$. On the other hand, it is easy to see that

$$\mathcal{R}\big(E, \mathcal{H}g_z^\epsilon\big) = -\int_{\partial D} \big(\nu \times \mathcal{H}g_z^\epsilon\big) \cdot \operatorname{curl} E \, \mathrm{d}s.$$

Combining the above results, we finally have that

$$\mathcal{R}\big(E, \mathcal{H}g_z^\epsilon\big) - \mathcal{R}(E, E_e(\cdot, z, q, k_b)) = -\int_{\partial D} \big(\nu \times \mathcal{H}g_z^\epsilon\big) \cdot \operatorname{curl} E \, \mathrm{d}s - W(x_0) + \mathbb{G}(z, x_0)p. \tag{34}$$

Now since $\big\|\mathcal{H}g_z^\epsilon\big\|_{H_{\mathrm{div}}^{-\frac{1}{2}}(\partial D)} < C$ there exists a subfamily, still denoted by $\mathcal{H}g_z^\epsilon$, that converges weakly to a $V \in H_{\mathrm{div}}^{-\frac{1}{2}}(\partial D)$ in the duality pairing between $H_{\mathrm{div}}^{-\frac{1}{2}}(\partial D)$ and $H_{\mathrm{curl}}^{-\frac{1}{2}}(\partial D)$ as $\epsilon \to 0$. Let us set

$$\tilde{W}(x_0) = \lim_{\epsilon \to 0} \mathcal{R}\big(E, \mathcal{H}g_z^\epsilon\big) = -\int_{\partial D} (\nu \times V) \cdot \operatorname{curl} E(\cdot, x_0, p) \, \mathrm{d}s, \qquad x_0 \in \Lambda.$$

From (33) we now have that

$$\tilde{W}(x_0) = W(x_0) + \mathbb{G}(z, x_0)p \qquad x_0 \in \Lambda. \tag{35}$$

Since $\tilde{W}(x_0)$ and $W(x_0)$ can be continued as radiating solutions to

$$\operatorname{curl}_{x_0} \operatorname{curl}_{x_0} E^s(x, x_0, p) - k^2 n(x_0) E^s(x, x_0, p) = 0$$

outside the domain bounded by Λ we deduce by uniqueness and the unique continuation principle that (35) holds true in $\mathbb{R}^3 \backslash (\overline{D} \cup \{z_0\})$. We now arrive at a contradiction by letting $x_0 \to z$. Hence $\mathcal{H}g_z^\epsilon$ is unbounded in the $H(D, \operatorname{curl})$ norm as $\epsilon \to 0$, which proves the theorem. □

Next, we turn to the investigation of the solvability of

$$\mathcal{R}(E, A\varphi) = \mathcal{R}(E, E_e(\cdot, z, q, k_b)) \tag{36}$$

with respect to φ where $E_e(\cdot, z, q, k_b)$ is given by (23) and $A\varphi$ is the single layer potential with density $\varphi \in L^2_{\mathrm{div}}(\tilde{\Lambda})$ given by (22). In order to carry out the analysis of (30) to the case of (36) we need the following key lemma.

Lemma 4.4. *Assume that k is not a Maxwell eigenvalue for D. Then the set* $\{A\varphi, \varphi \in H_{\mathrm{div}}^{-\frac{1}{2}}(\tilde{\Lambda})$ *is dense in* $H(\mathit{curl}, D)$.

Proof. Making use of the well-posedness of

$$\operatorname{curl}\operatorname{curl} W - k^2 n_b W = 0 \quad \text{in } D \tag{37}$$

$$\nu \times W = f \quad \text{on } \partial D \tag{38}$$

with $f \in H_{\mathrm{div}}^{-\frac{1}{2}}(\partial D)$, it suffices to show that $\nu \times A\varphi|_{\partial D}$ for all $\varphi \in H_{\mathrm{div}}^{-\frac{1}{2}}(\tilde{\Lambda})$ is dense in $H_{\mathrm{div}}^{-\frac{1}{2}}(\partial D)$. To this end, let $\psi \in H_{\mathrm{curl}}^{-\frac{1}{2}}(\partial D)$ and look at the dual operator $A^* : H_{\mathrm{curl}}^{-\frac{1}{2}}(\partial D) \to H_{\mathrm{div}}^{-\frac{1}{2}}(\Gamma)$ such that

$$\langle \nu \times A\varphi, \psi \rangle_{\partial D} = \langle \varphi, A^* \psi \rangle_{\tilde{\Lambda}}$$

where $\langle\cdot,\cdot\rangle$ denotes the $H_{\mathrm{div}}^{-\frac{1}{2}}, H_{\mathrm{curl}}^{-\frac{1}{2}}$ duality pairing. By changing the order of integration one can show that for $\psi \in H_{\mathrm{div}}^{-\frac{1}{2}}(\partial D)$

$$(A^*\psi)(y) = \nu(y) \times \left(\mathrm{curl}_y \mathrm{curl}_y \int_{\partial D} \psi(x)\Phi(x, y)\, \mathrm{d}s(x)\right) \times \nu(y), \qquad y \in \tilde{\Lambda}$$

where ν is the unit outward normal to $\tilde{\Lambda}$. Now, since k_b is not a Maxwell eigenvalue for D, we conclude that A^* is injective, whence $\left\{\nu \times A\varphi|_{\partial D} : \varphi \in H_{\mathrm{div}}^{-\frac{1}{2}}(\tilde{\Lambda})\right\}$ is dense in $H_{\mathrm{div}}^{-\frac{1}{2}}(\partial D)$. □

Now in exactly the same way as in theorem 4.3 we can prove the following result concerning a (approximate) solution to (36).

Theorem 4.5. *The results of theorem 4.3 remain valid if we replace the operator $\mathcal{H}$ by A and the space $L_t^2(S^2)$ by $H_{\mathrm{div}}^{-\frac{1}{2}}(\tilde{\Lambda})$.*

Remark 4.1. As noted in the proof of theorem 4.3, there are many choices of the parametrization of the gap reciprocity functional $\mathcal{R}(E, W)$ in terms of $W := F\psi$ where $F\psi \in \mathbb{H}(\Omega)$ with density function ψ in a Hilbert space H. The only requirement is that $\{F\psi, \psi \in H\}$ form a dense subset of $\mathbb{H}(\Omega)$.

The behaviour of the approximate solutions to (30) and (36) provided by theorems 4.3 and 4.5, respectively, can be used in the same way as in the standard linear sampling method to characterize the scattering object D.

4.2. The reciprocity gap functional for an inhomogeneous medium

Let now $E = E(\cdot, x_0, p) = E^s(\cdot, x_0, p) + \mathbb{G}(\cdot, x_0)p$ for $x_0 \in \Lambda$ be the total electric field corresponding to the scattering problem (SIM).

The *interior transmission problem*

$$\mathrm{curl}\,\mathrm{curl}\, E_0 - k^2 n_b E_0 = 0 \quad \text{in } D \tag{39}$$

$$\mathrm{curl}\,\mathrm{curl}\, E^{\mathrm{int}} - k^2 N(x) E^{\mathrm{int}} = 0 \quad \text{in } D \tag{40}$$

$$\nu \times E^{\mathrm{int}} - \nu \times E_0 = f \quad \text{on } \partial D \tag{41}$$

$$\nu \times \mathrm{curl}\, E^{\mathrm{int}} - \nu \times \mathrm{curl}\, E_0 = h \quad \text{on } \partial D. \tag{42}$$

plays an important role in the study of the inverse problem. In [23] it is shown that provided that $\mathrm{Re}(N - n_b I)^{-1}$ is bounded below, for given $f \in H^{\frac{3}{2}}(D)$ and $h \in H^{\frac{1}{2}}(\partial D)$ there exists a solution $E \in L^2(D)$ and $E_0 \in L^2(D)$ such that $E - E_0 \in H^2(D)$ provided that uniqueness holds. Furthermore, the solution depends continuously in $L^2(D)$ on the boundary data f and h in their respective norms. The values of k for which the homogeneous interior transmission problem ($f = h = 0$) has a nontrivial solution are called *transmission eigenvalues*. In particular, in [23] it is also shown that if $\mathrm{Im}(N - n_b I)^{-1} < 0$ then transmission eigenvalues do not exist.

Lemma 4.6. *Assume that k is not a transmission eigenvalue for D. Then the operator $R : \mathbb{H}(\Omega) \to L_t^2(\Lambda)$ defined by (20) is injective.*

Proof. From (20), $RW = 0$ means $\mathcal{R}(E(\cdot, x_0, p(x_0)), W) = 0$ for all $(x_0, p(x_0))$. Integrating by parts, we have that

$$0 = \int_\Gamma (\nu \times E) \cdot \operatorname{curl} W - (\nu \times W) \cdot \operatorname{curl} E \, ds \tag{43}$$
$$= \int_{\partial D} (\nu \times E) \cdot \operatorname{curl} W - (\nu \times W) \cdot \operatorname{curl} E \, ds = k^2 \int_D (N - n_b I) W \cdot E \, dx.$$

Now let $\tilde{E} \in H_{\text{loc}}(\mathbb{R}^3)$ be the unique solution to (see [28])

$$\begin{aligned} &\operatorname{curl}\operatorname{curl} \tilde{E} - k^2 N(x) \tilde{E} = k^2 (N(x) - n_b(x) I) W \quad \text{in } \mathbb{R}^3 \\ &\lim_{r \to \infty} (\operatorname{curl} \tilde{E} \times x - \mathrm{i} k r \tilde{E}) = 0. \end{aligned} \tag{44}$$

Here $N(x)$ in $\mathbb{R}^3 \backslash \overline{D}$ is equal to $n_b(x)$ and $N(x) - n_b(x) = N(x) - n_b$ in D where n_b is the constant index of refraction inside Ω. Now (43) can be rewritten as

$$\int_D (\operatorname{curl}\operatorname{curl} \tilde{E} - k^2 N \tilde{E}) \cdot (E^s + \mathbb{G}(\cdot, x_0) p) \, dx = 0. \tag{45}$$

Using integration by parts, the equation satisfied by the scattered field E^s and the fact that E^s and $\tilde{E}$ are radiating solutions, we obtain

$$\begin{aligned} \int_D (\operatorname{curl}\operatorname{curl} \tilde{E} - k^2 N \tilde{E}) \cdot E^s \, dx &= \int_D (\operatorname{curl}\operatorname{curl} E^s - k^2 N E^s) \cdot \tilde{E} \, dx \\ &\quad + \int_{\partial D} [(\nu \times E^s) \cdot \operatorname{curl} \tilde{E} - (\nu \times \tilde{E}) \cdot \operatorname{curl} E^s] \, ds \\ &= k^2 \int_D (N - n_b I) \mathbb{G}(\cdot, x_0) p \, ds. \end{aligned} \tag{46}$$

On the other hand,

$$\begin{aligned} \int_D \operatorname{curl}\operatorname{curl} \tilde{E} \cdot \mathbb{G}(\cdot, x_0) p &= \int_D \operatorname{curl}\operatorname{curl} \mathbb{G}(\cdot, x_0) p \cdot \tilde{E} \, dx \\ &\quad + \int_{\partial D} [(\nu \times \mathbb{G}(\cdot, x_0) p) \cdot \operatorname{curl} \tilde{E} - (\nu \times \tilde{E}) \cdot \operatorname{curl} \mathbb{G}(\cdot, x_0) p] \, ds. \end{aligned} \tag{47}$$

Substituting (47) and (46) into (45) and using the Stratton–Chu representation formula outside D [28] we obtain

$$\begin{aligned} 0 = \int_D \tilde{E} (\operatorname{curl}\operatorname{curl} \mathbb{G}(\cdot, x_0) p - k^2 n_b \mathbb{G}(\cdot, x_0) p) \, dx \\ + \int_{\partial D} [(\nu \times \mathbb{G}(\cdot, x_0) p) \cdot \operatorname{curl} \tilde{E} - (\nu \times \tilde{E}) \cdot \operatorname{curl} \mathbb{G}(\cdot, x_0) p] = p \cdot \tilde{E}(x_0) \end{aligned}$$

since

$$\operatorname{curl}\operatorname{curl} \mathbb{G}(\cdot, x_0) p - k^2 n_b \mathbb{G}(\cdot, x_0) p = 0 \qquad \text{in } D.$$

Hence, since p is an arbitrary polarization in the tangent plane to Λ at x_0, we obtain that $\nu \times \tilde{E}(x_0) = 0$ for $x_0 \in \Lambda$. Furthermore, since $\tilde{E}$ is a radiating solution to $\operatorname{curl}\operatorname{curl} \tilde{E} - k^2 n(x) \tilde{E} = 0$ outside the domain bounded by Λ and satisfies $\nu \times \tilde{E} = 0$ on Λ, we can conclude by the uniqueness theorem for scattering by a perfect conductor that $\tilde{E} = 0$ outside the domain bounded by Λ. Finally, from the unique continuation principle we have that $\tilde{E} = 0$ outside D as well. Therefore, $E_0 := W$ and $E^{\text{int}} := \tilde{E} + W$ satisfy the homogeneous interior transmission problem, whence by the assumption that k is not a transmission eigenvalue we finally obtain that $W = 0$ in D. This proves the lemma. □

Remark 4.2. The proof of lemma 4.6 adapted to the case of the Helmholtz equation can replace the proof of the same result in the scalar case in [12] where the Runge approximation property for elliptic equations is used.

Lemma 4.7. *Assume that k is not a transmission eigenvalue. Then the range of $R : \mathbb{H}(\Omega) \to L_t^2(\Lambda)$ defined by (20) is dense.*

Proof. The proof follows the proof of lemma 4.2 with slight modifications. In particular, W and $\mathcal{E}$ defined by (28) with $E(\cdot, x_0, p)$ being the total field corresponding to (SIM) satisfy the interior transmission problem (39)–(42) with $E_0 := W$ and $E := \mathcal{E}$, and (29) needs to be replaced by an equation of type (43) for W and $\mathcal{E}$.

We are now ready to study the solvability of equations (30) and (36) in the case of the scattering problem for an inhomogeneous anisotropic scatterer. To fix our ideas, we first consider

$$\mathcal{R}(E, \mathcal{H}g) = \mathcal{R}(E, E_e(\cdot, z, q, k_b))$$

where $\mathcal{H}g$ is the electric Herglotz function with $g \in L_t^2(S^2)$. □

Theorem 4.8. *Assume that k is not a transmission eigenvalue for D and let $E = E(\cdot, x_0, p)$ and $H = 1/\mathrm{ik}\,\mathrm{curl}\,E$ be the total electric and magnetic fields, respectively, corresponding to the scattering problem (SIM). Then we have the following:*

(i) For $z \in D$ and a given $\epsilon > 0$, there exists a $g_z^\epsilon \in L_t^2(S^2)$ such that

$$\left\|\mathcal{R}\left(E, \mathcal{H}g_z^\epsilon\right) - \mathcal{R}(E, E_e(\cdot, z, q, k_b))\right\|_{L_t^2(\Lambda)} < \epsilon$$

and the corresponding electric Herglotz wavefunction $\mathcal{H}g_z^\epsilon$ converges in the $L^2(D)$ norm to E_0 as $\epsilon \to 0$ where (E^{int}, E_0) is the solution of (39)–(42) with $f := E_e(\cdot, z, q, k_b)$ and $h = \nu \times \mathrm{curl} E_e(\cdot, z, q, k_b)$.

Parts (ii) and (iii) of theorem 4.3 are also valid in this case.

Proof. Consider $z \in D$ and let E_0 and E^{int} be the solution to the interior transmission problem (39)–(42) with $f := E_e(\cdot, z, q, k_b)$ and $h = \nu \times \mathrm{curl}\, E_e(\cdot, z, q, k_b)$. Since $W \in \mathbb{H}(\Omega)$ and $E_e(\cdot, z, q, k_b)$ satisfy $\mathrm{curl}\,\mathrm{curl}\, W - k_b W = 0$ in $\Omega \backslash \overline{D}$, integrating by parts and using the equations satisfied by the total electric field we have that

$$\mathcal{R}(E, W) = k^2 \int_D (N - n_1 I) W \cdot E \, \mathrm{d}x. \tag{48}$$

If W coincides with E_0 in D then since E and E^{int} satisfy the same equation in D we obtain that

$$\mathcal{R}(E, W) = \mathcal{R}(E, E_e(\cdot, z, q, k_b)).$$

But it is, in general, impossible to find a function $W \in \mathbb{H}(\Omega)$ such that $W|_D$ and E^{int} satisfy the interior transmission problem (39)–(42) with $f := E_e(\cdot, z, q, k_b)$ and $h = \nu \times \mathrm{curl}\, E_e(\cdot, z, q, k_b)$. However, in lemma 4.3 in [23], it is shown that the set $\{\mathcal{H}g, g \in L_t^2(S^2)\} \subset \mathbb{H}(\Omega)$ is a dense subset of

$$\{U \in L^2(D), \mathrm{curl}\,\mathrm{curl}\, U - k^2 n_b U = 0 \text{ in the distributional sense}\}.$$

Hence for every $\epsilon > 0$ we can find a $g_z^\epsilon \in L_t^2(S^2)$ such that

$$\left\|\mathcal{R}\left(E, \mathcal{H}g_z^\epsilon\right) - k^2 \int_D (N - n_1 I) E_0 \cdot E \, \mathrm{d}x\right\|_{L_t^2(\Lambda)} < \epsilon,$$

whence by the above discussion

$$\left\|\mathcal{R}\left(E, \mathcal{H}g_z^\epsilon\right) - \mathcal{R}(E, E_e(\cdot, z, q, k_b))\right\|_{L_t^2(\Lambda)} < \epsilon.$$

Furthermore, by construction, $\mathcal{H}g_z^\epsilon$ converges to E_0 in the $L^2(D)$ norm as $\epsilon \to 0$. Next we observe that $\tilde{E} = E_e(\cdot, z, q, k_b)$ in $\mathbb{R}^3\backslash\overline{D}$ and $\tilde{E} = (E^{\text{int}} - E_0)$ in D satisfies

$$\operatorname{curl}\operatorname{curl}\tilde{E} - k^2 N\tilde{E} = k^2(N - n_b I)W \quad \text{in } \mathbb{R}^3 \qquad \lim_{r\to\infty}(\operatorname{curl}\tilde{E} \times x - \mathrm{i}kr\tilde{E}) = 0$$

where again $N(x)$ in $\mathbb{R}^3\backslash\overline{D}$ is equal to $n_b(x)$ and $N(x) - n_b(x) = N(x) - n_b$ in D. From the well-posedness of the direct scattering problem for an inhomogeneous medium [28], we have that

$$\|E_e(\cdot, z, q, k_b)\|_{H(\operatorname{curl}, \mathbb{R}^3\backslash\overline{D}\cap B_R)} < \|E_0\|_{L^2(D)}.$$

Hence, due to the singularity of the electric dipole, we can conclude that $\|E_0\|_{L^2(D)} \to \infty$ as $z \to \partial D$ and so does $\left\|\mathcal{H}g_z^\epsilon\right\|_{L(D)}$ and $\left\|g_z^\epsilon\right\|_{L_t^2(S^2)}$.

The last part of the theorem for $z \in \mathbb{R}^3\backslash\overline{D}$ can be proved in exactly the same way as in theorem 4.3. Note that now (34) becomes

$$\mathcal{R}\left(E, \mathcal{H}g_z^\epsilon\right) - \mathcal{R}(E, E_e(\cdot, z, q, k_b)) = k^2 \int_D (N - n_b I)\mathcal{H}g_z^\epsilon \cdot \operatorname{curl} E \, \mathrm{d}x - W(x_0) + \mathbb{G}(z, x_0)p$$

and a contradiction can be arrived at in the same way by using the weak convergence of $\mathcal{H}g_z^\epsilon$ to a function $V \in L^2(D)$ as $\epsilon \to 0$. □

Finally, we can prove the same result for a solution to

$$\mathcal{R}(E, A\varphi) = \mathcal{R}(E, E_e(\cdot, z, q, k_b))$$

where the potential $A\varphi$ is given by (22). In particular, we can prove the following theorem:

Theorem 4.9. *The results of theorem 4.8 remain valid if we replace the operator $\mathcal{H}$ by A and the space $L_t^2(S^2)$ by $L_{\text{div}}^2(\tilde{\Lambda})$.*

Proof. The proof is the same as the proof of theorem 4.8. The only piece missing is to show that $\{A\varphi, \varphi \in L_{\text{div}}^2(\tilde{\Lambda})\} \subset \mathbb{H}(\Omega)$ is dense in the set

$$\{U \in L^2(D), \operatorname{curl}\operatorname{curl} U - k^2 n_b U = 0 \text{ in the distributional sense}\}$$

with respect to the $L^2(D)$ norm. But this can be done in the same way as in lemma 4.3 in [23], where instead of the functions M_n one uses the radiating solutions N_n (see theorem 6.24 in [15]).

Finally, we note that the same remark stated at the end of section 3 is valid for the regularized solution of (24) and (25). In particular, it is not known theoretically that this regularized solution behaves similarly to the ϵ solution as described in theorems 4.8 and 4.9.

We end this section by remarking that the sampling method based on the reciprocity gap functional can also be used if the medium inside Ω is heterogeneous. However, in this case one needs to compute Green's tensor for the medium inside Ω only. □

5. Numerical validation

We now discuss the performance of the classical linear sampling method (LSM) that has been reviewed in section 3 and the sampling method based on the reciprocity rap functional (RG-LSM), discussed in section 4, for which we shall restrict ourselves to the case of perfectly conducting scatterers and will use simple layer potentials (22) as parametrization, that is, we implement only (25). We refer to [12] for a comparison between the numerical performance of (24) and (25). For instance, it is shown that the reconstructions using (25) are more stable with respect to absorption.

5.1. Numerical discretization

For both methods, and after numerical discretization, one ends up with a linear system to solve of the form

$$\mathcal{A}\phi(z,q) = F(z,q) \tag{49}$$

where z denotes a sampling point in the probed region and $q \in \mathbb{R}^3$ is an arbitrary polarization vector. The expression and the size of the matrix $\mathcal{A}$ and the right-hand side $F(z,q)$ depend on the method used.

Let $(s_i)_{i=1,N_s}$ denote the source locations on Λ and $(x_i)_{i=1,N_0}$ denote the measurement points on Γ. For y belonging to Λ or Γ, we denote by $(\tau_1(y), \tau_2(y))$ a pair of orthogonal unit tangent vectors (to the surface) at y.

(1) For the LSM, the matrix $\mathcal{A}$ is then a $2N_0 \times 2N_s$ matrix whose entries are defined by

$$\mathcal{A}_{i,j} = w_j E^s(x_i, s_j, \tau_1(s_j)), \qquad \mathcal{A}_{i,j+N_s} = w_j E^s(x_i, s_j, \tau_2(s_j)),$$

for $1 \leqslant i \leqslant N_0$ and $1 \leqslant j \leqslant N_s$, and

$$\mathcal{A}_{i+N_0,j} = \mathcal{A}_{i,j},$$

for $1 \leqslant i \leqslant N_0$ and $1 \leqslant j \leqslant 2N_s$, where the weights $(w_i)_{i=1,N_s}$ correspond to a quadrature rule associated with the nodes $(s_i)_{i=1,N_s}$. For instance, if the $(s_i)_{i=1,N_s}$ are the vertices of a triangular mesh $\mathcal{T}$ of Λ then the quadrature rule associated with a linear interpolation corresponds to

$$w_j = \frac{1}{3} \sum_{T \in \mathcal{T}, T \ni s_j} |T|. \tag{50}$$

The right-hand side in this case is

$$F_i(z,q) = (\mathbb{G}(x_i,z)q) \cdot \tau_1(x_i) \qquad \text{and} \qquad F_{i+N_0}(z,q) = (\mathbb{G}(x_i,z)q) \cdot \tau_2(x_i),$$

for $1 \leqslant i \leqslant N_0$.

(2) For the second method, RG-LSM, one also needs to mesh the surface $\tilde{\Lambda}$ of the simple layer potential. Similarly as above, we denote by $(\tilde{s}_i)_{i=1,\tilde{N}_s}$ the vertices of a triangular mesh $\tilde{\mathcal{T}}$ of $\tilde{\Lambda}$ and by $(\tilde{w}_i)_{i=1,\tilde{N}_s}$ the corresponding weights (similarly as in (50)). Then the matrix $\mathcal{A}$ is a $2N_s \times 2\tilde{N}_s$ matrix whose entries are defined by

$$\mathcal{A}_{i,j} = \tilde{w}_j \mathcal{R}(E(\cdot, s_i, \tau_1(s_i)), E_e(\cdot, \tilde{s}_j, \tau_1(\tilde{s}_j), k_b)),$$
$$\mathcal{A}_{i,j+\tilde{N}_s} = \tilde{w}_j \mathcal{R}(E(\cdot, s_i, \tau_1(s_i)), E_e(\cdot, \tilde{s}_j, \tau_2(\tilde{s}_j), k_b)),$$

for $1 \leqslant i \leqslant N_s$ and $1 \leqslant j \leqslant \tilde{N}_s$, and

$$\mathcal{A}_{i+N_s,j} = \tilde{w}_j \mathcal{R}(E(\cdot, s_i, \tau_2(s_i)), E_e(\cdot, \tilde{s}_j, \tau_1(\tilde{s}_j), k_b)),$$
$$\mathcal{A}_{i+Ns,j+\tilde{N}_s} = \tilde{w}_j \mathcal{R}(E(\cdot, s_i, \tau_2(s_i)), E_e(\cdot, \tilde{s}_j, \tau_2(\tilde{s}_j), k_b)),$$

for $1 \leqslant i \leqslant N_s$ and $1 \leqslant j \leqslant \tilde{N}_s$. The right-hand side in this case is

$$F_i(z,q) = \mathcal{R}(E(\cdot, s_i, \tau_1(s_i)), E_e(\cdot, z, q, k_b))$$
$$F_{i+N_s}(z,q) = \mathcal{R}(E(\cdot, s_i, \tau_2(s_i)), E_e(\cdot, z, q, k_b))$$

for $1 \leqslant i \leqslant N_s$. The evaluation of $\mathcal{R}$ uses the data on Γ and is achieved by using a quadrature rule associated with a linear interpolation as in (50).

5.2. Inversion scheme

Since equation (49) corresponds to the discretization of an ill-posed linear equation, a regularization is needed to compute an approximate solution. As in [13], we choose to use Tikhonov regularization with a regularization parameter computed via the Morozov discrepancy principle. To visualize the scatterer, we evaluate the criteria (similar to that in [13])

$$G(z) = \frac{\|F(z, q_1)\|}{\|\varphi(z, q_1)\|} + \frac{\|F(z, q_2)\|}{\|\varphi(z, q_2)\|} + \frac{\|F(z, q_3)\|}{\|\varphi(z, q_3)\|} \tag{51}$$

where $q_1 = (1, 0, 0)$, $q_2 = (0, 1, 0)$ and $q_3 = (0, 0, 1)$ which corresponds to a special choice of three independent polarizations and where a scaling with the norm of the right-hand side is added [12]. We then plot the isosurface

$$\mathcal{G}(z) = C \max(G(z)) \tag{52}$$

where C is a parameter. In order to get a good approximation of the probed geometry, the value of this parameter should be chosen so that $C \max(G(z))$ is in the transition region between small and large values of $\mathcal{G}(z)$. One can imagine an automatic evaluation of the 'best value' based on the analysis of the gradient of these criteria, but this issue is beyond the scope of the present work.

Our experience suggests that values of C between 0.4 and 0.5 usually give reasonable reconstructions. We give in the following examples the reconstructions that correspond to different values of this parameter (within the admissible region). We refer to [11, 17, 27] for a related study on the choice of C. Let us finally mention the strategy for choosing C suggested in [18] where the 'best choice range' for C is determined first by using a toy example, and then this choice is used for other reconstructions. The best choice of C turns out to be consistent for different obstacles, as our examples show.

5.3. Numerical examples

We shall conclude this work by giving some numerical examples using synthetic data that illustrate the performance of the two sampling methods described above. We present here numerical experiments for the case of a perfectly conducting obstacle buried in the earth. In particular, we assume that the background is a two-layered medium, the upper one models the air where the wave number is real and equal to k ($n(x) = 1$) and the lower one models the earth with the constant index of refraction n ($n_b = n$). The scatterer is a perfect conductor buried in the earth.

We restrict ourselves to the cases where the interface is straight. In that case, one can derive an integral representation for the Green tensor of the background medium in terms of Bessel-like transforms [28]. Therefore one has access to a reasonably cheap evaluation of the background Green tensor required by the classical LSM algorithm. We remind the reader that this is not needed by the second method and therefore the examples presented here may not be fully representative of the potential of this method.

Let $\lambda = 2\pi/k$ denote the wavelength in air. The data correspond to sources uniformly distributed on a squared horizontal plate of size $3\lambda \times 3\lambda$ at $z = \lambda/2$. Using the previous notation, this corresponds to

$$\Lambda = [-1.5\lambda, 1.5\lambda] \times [-1.5\lambda, 1.5\lambda] \times \{\lambda/2\}.$$

The number of source points is $N_s = 25 \times 25$ and for each point source two horizontal polarizations are used. Consequently, 1250 incident waves are used.

The measurement location depends on the method used. The measurements are synthetically generated using CESC software: a solver for electromagnetic scattering problems

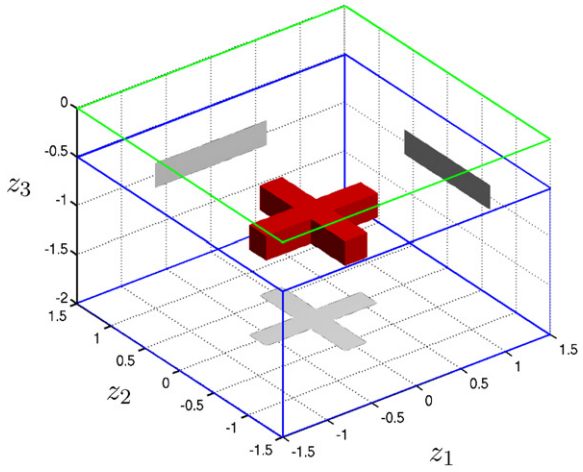

Figure 3. Exact geometry of the perfect conductor in the first example. The interface earth–air is at $z_3 = 0$. The box indicates the boundary of the probed region.

developed at CERFACS. The perfectly conducting case is treated by solving the electric field integral equation, whose unknown is the electric current on the surface of the scatterer. The numerical discretization is based on a triangular meshing of the surface and the use of Raviart–Thomas's finite elements of the lowest degree.

Measurements for the LSM. In the case of the LSM, we take $\Gamma = \Lambda$ and the number of measurements is equal to the number of incident waves: for each incident wave we measure the tangential components of the scattered field at the location of the 625 source points.

Measurements for the RG-LSM. In the case of the second method, the measurement surface needs to be the boundary of a homogeneous domain containing the scatterer. Therefore Γ cannot be the same as Λ. It is also not reasonable (at least for the above-mentioned application) to measure all around the target. However, it is easy to show in the case of a layered medium that one can also take Γ to be the interface between the two media. Now if one assumes that there is enough absorption inside the earth, one can restrict the measurements (up to a small error) to a bounded region of this interface where the wave is not sufficiently damped. In the following experiments, this region is chosen to be

$$[s_{i,x} - 2\lambda, s_{i,x} + 2\lambda] \times [s_{i,y} - 2\lambda, s_{i,y} + 2\lambda] \times \{0\}$$

where s_i denotes the location of the point source. The tangential electric and magnetic fields are evaluated on a uniformly distributed 40×40 grid of this region. It is noted that the number of data used here is substantially higher than that for the LSM. However, an increase in the number of data for the LSM (by increasing the aperture) did not substantially improve the results. On the other hand, we did not optimize the number of data required to sufficiently accurately evaluate the reciprocity gap functional. We used

$$\tilde{\Lambda} = [-\lambda, \lambda] \times [-\lambda, \lambda] \times \{\lambda/2\}.$$

as the surface for the simple layer potential with a uniform 25×25 grid.

Using these data we get an execution time on an SGI ORIGIN 2000 computer for one sampling point (that is roughly the same for the two methods) that is less than 4 s.

5.3.1. Example 1. The first example is depicted in figure 3 and corresponds to a perfectly conducting cross.

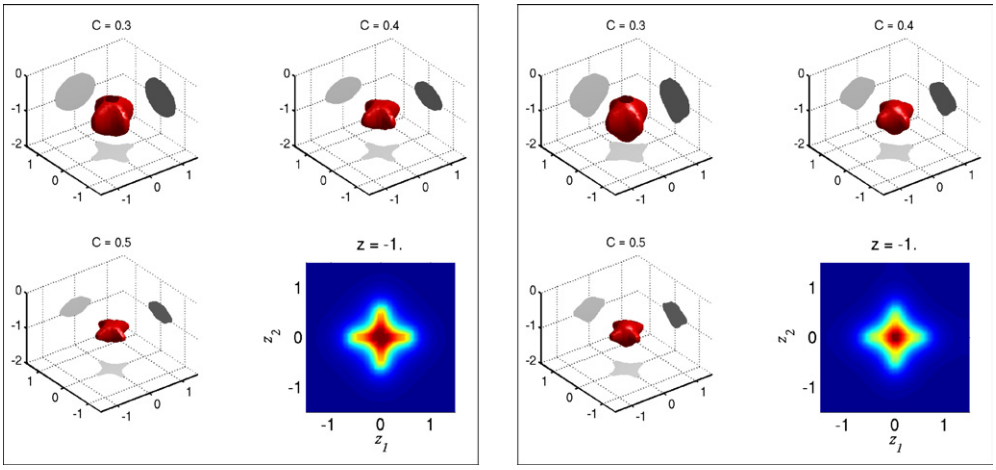

Figure 4. Reconstructed geometries for $n = 2 + 0.1\mathrm{i}$ and an added 1% random noise (see exact geometry in figure 3). The wavelength in air is $\lambda = 1$. LSM: left four figures; RG-LSM: right four figures. Each 3D plot corresponds to a different choice of the isosurface value. The 2D plot corresponds to a horizontal cross section of $\mathcal{G}$ at $z_3 = -1$.

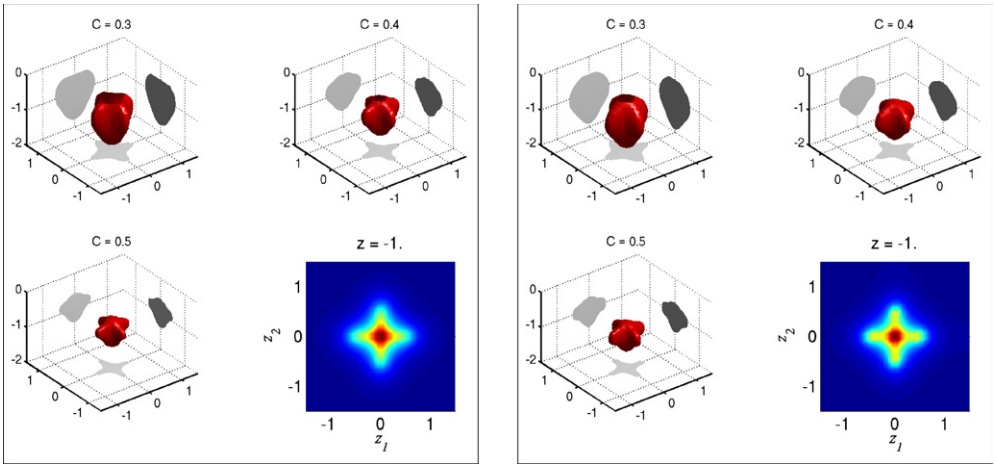

Figure 5. Reconstructed geometries for $n = 2 + 0.5\mathrm{i}$ and an added 1% random noise (see exact geometry in figure 3). The wavelength in air is $\lambda = 1$. LSM: left four figures; RG-LSM: right four figures. Each 3D plot corresponds to a different choice of the isosurface value. The 2D plot corresponds to a horizontal cross section of $\mathcal{G}$ at $z_3 = -1$.

For the inversion, we used a wavelength in air of $\lambda = 1$ which is roughly the horizontal size of the cross. The wavelength inside the earth is smaller since we took the real part of its index equal to 2. We present in the following the results of three inversions where we varied the absorption in the medium. We respectively used $n = 2 + 0.1\mathrm{i}$, $n = 2 + 0.5\mathrm{i}$ and $n = 2 + \mathrm{i}$ and the respective results are shown in figures 4, 5 and 6. In each figure the results given by LSM are presented in the left box and those from RG-LSM in the right box. We observe that the quality of the reconstruction is roughly the same when the absorption is sufficiently high: $n = 2 + 0.5\mathrm{i}$ and $n = 2 + \mathrm{i}$, which can be explained by the fact that in these cases the measurements for RG-LSM satisfy the above-mentioned requirements. When $n = 2 + 0.1\mathrm{i}$

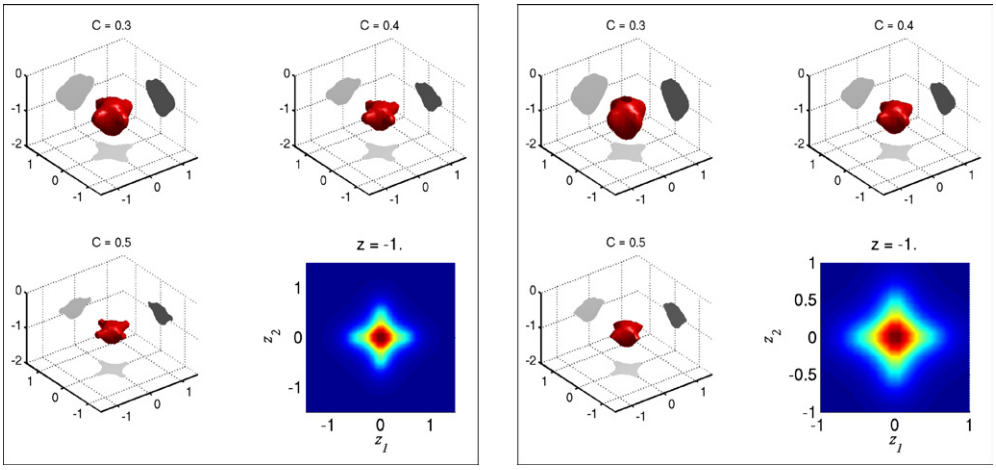

Figure 6. Reconstructed geometries for $n = 2 + 1.0\mathrm{i}$ and an added 1% random noise (see exact geometry in figure 3). The wavelength in air is $\lambda = 1$. LSM: left four figures; RG-LSM: right four figures. Each 3D plot corresponds to a different choice of the isosurface value. The 2D plot corresponds to a horizontal cross section of $\mathcal{G}$ at $z_3 = -1$.

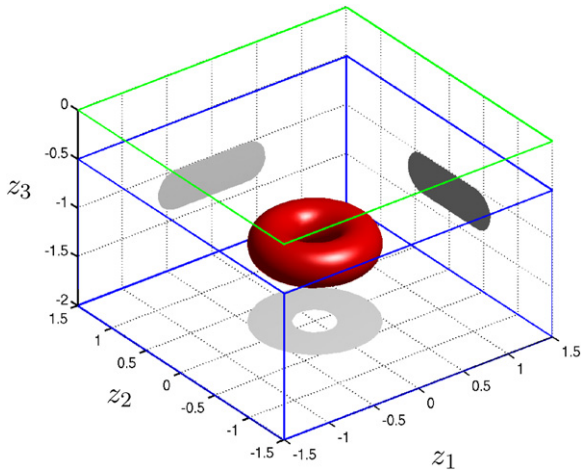

Figure 7. Exact geometry of the perfect conductor in the second example. The interface earth–air is at $z_3 = 0$. The box indicates the boundary of the probed region.

these requirements are violated to some extent which may explain why the LSM works better in this case. The 2D plots in these figures correspond to the values of $\mathcal{G}$ at a depth that coincides with the mean cross section of the scatterer. These plots and also the projections on the x–y plane of the reconstructed geometry constitute, in our opinion, what one can reasonably expect to get from an imaging technique with data given as above. In this respect both methods give satisfactory reconstruction.

5.3.2. Example 2. The second example is a perfectly conducting torus as shown in figure 7.

For the inversion, we used a wavelength in air of $\lambda = 1$ which is roughly the exterior diameter of the torus. We present in the following figures the results of two inversions where

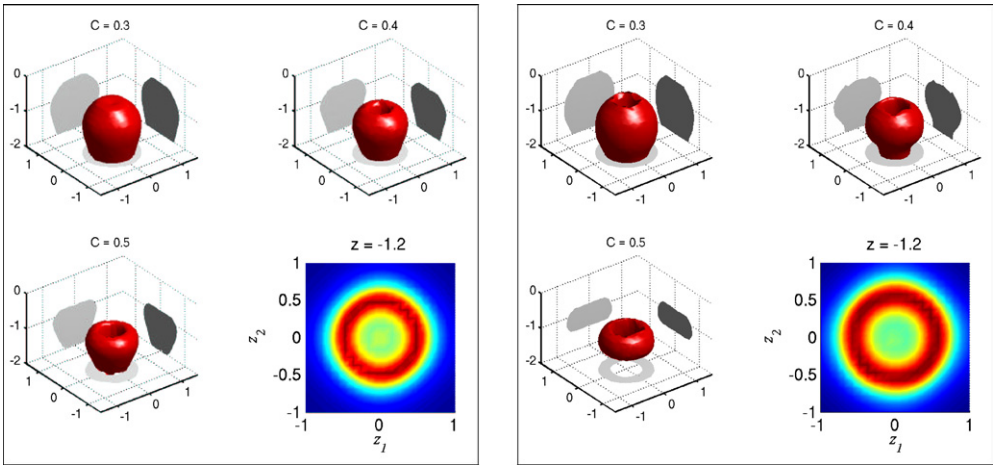

Figure 8. Reconstructed geometries for $n = 2 + 0.5\mathrm{i}$ and an added 1% random noise (see exact geometry in figure 7). The wavelength in air is $\lambda = 1$. LSM: left four figures; RG-LSM: right four figures. Each 3D plot corresponds to a different choice of the isosurface value. The 2D plot corresponds to a horizontal cross section of $\mathcal{G}$ at $z_3 = -1.2$.

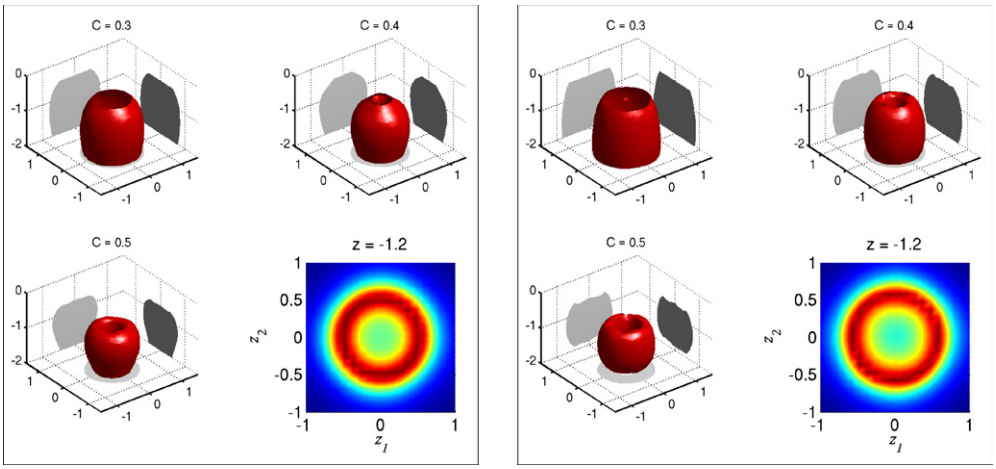

Figure 9. Reconstructed geometries for $n = 2 + 0.5\mathrm{i}$ and an added 5% random noise (see exact geometry in figure 7). The wavelength in air is $\lambda = 1$. LSM: left four figures; RG-LSM: right four figures. Each 3D plot corresponds to a different choice of the isosurface value. The 2D plot corresponds to a horizontal cross section of $\mathcal{G}$ at $z_3 = -1.2$.

the index of the earth is $n = 2 + 0.5\mathrm{i}$ and where we varied the added noise: 1% for the first example (figure 8) and 5% for the second example (figure 9). We observe a good stability of the localization and the reconstruction of the shape in horizontal directions, as attested by the 2D plots and the projections shown in these figures.

Acknowledgments

The first author gratefully acknowledges the support of her research by the Air Force Office of Scientific Research under grant no FA9550-05-1-0127. The authors would like to thank the CINES (Centre Informatique National de l'Enseignement Supérieur, France) for giving them

the opportunity to use their SGI ORIGIN 2000 computers and would like to thank Francis Collino for his precious help in setting up the forward solver for two-layered background.

References

[1] Andrieux S and Ben Abda A 1996 Identification of planar cracks by complete over-determined data: inversion formulae *Inverse Problems* **12** 553–63

[2] Arens T 2004 Why linear sampling method works *Inverse Problems* **20** 163–73

[3] Baum C 1999 *Detection and Identification of Visually Obscured Targets* (London: Taylor and Francis)

[4] Bonnet M and Constantinescu A 2005 Inverse problems in elasticity *Inverse Problems* **21** R1–R50

[5] Buffa A and Ciarlet P Jr 2001 On traces for functional spaces related to Maxwell's equations: I. An integration by parts formula in Lipschitz polyhedra *Math. Methods Appl. Sci.* **24** 9–30

[6] Buffa A, Costabel M and Schwab C 2002 Boundary element methods for Maxwell's equations on non-smooth domains *Numer. Math.* **92** 679–710

[7] Cakoni F Recent developments in the qualitative approach to inverse scattering theory *J. Comput. Appl. Math.* at press

[8] Cakoni F and Colton D 2003 A uniqueness theorem for an inverse electromagnetic scattering problem in inhomogeneous anisotropic media *Proc. Edinburgh Math. Soc.* **46** 293–314

[9] Cakoni F and Colton D 2006 *Qualitative Methods in Inverse Scattering Theory* (Berlin: Springer)

[10] Cakoni F, Colton D and Haddar H 2002 The linear sampling method for anisotropic media *J. Comput. Appl. Math.* **146** 285–99

[11] Collino F, Fares M and Haddar H 2003 Numerical and analytical studies of the linear sampling method in electromagnetic scattering problems *Inverse Problems* **19** 1279–99

[12] Colton D and Haddar H 2005 An application of the reciprocity gap functional to inverse scattering theory *Inverse Problems* **21** 383–98

[13] Colton D, Haddar H and Monk P 2002 The linear sampling method for solving the electromagnetic inverse scattering problem *SIAM J. Sci. Comput.* **24** 719–31

[14] Colton D, Haddar H and Piana M 2003 The linear sampling method in inverse electromagnetic scattering theory *Inverse Problems* **19** S105–37

[15] Colton D and Kress R 1998 *Inverse Acoustic and Electromagnetic Scattering Theory* 2nd edn (Berlin: Springer)

[16] Colton D and Kress R 2001 On the denseness of Herglotz wave functions and electromagnetic Herglotz pairs in Sobolev spaces *Math. Methods Appl. Sci.* **24** 1289–303

[17] Colton D and Monk P Target identification of partially coated objects *IEEE Trans. Antennas Propag.* at press

[18] Colton D, Coyle J and Monk P 2000 Recent developments in inverse acoustic scattering theory *SIAM Rev.* **42** 369–414

[19] Coyle J 2000 An inverse electromagnetic scattering problem in a two-layered background *Inverse Problems* **16** 275–92

[20] Cutzach P and Hazard C 1998 Existence, uniqueness and analyticity properties for electromagnetic scattering in a two layered medium *Math. Methods Appl. Sci.* **21** 433–61

[21] Fara S N and Guzina B B 2004 A linear sampling method for near-field inverse problems in elastodynamics *Inverse Problems* **20** 713–36

[22] Gebauer B, Hanke M, Kirsch A, Muniz W and Schneider C 2005 A sampling method for detecting buried objects using electromagnetic scattering *Inverse Problems* **21** 2035–50

[23] Haddar H 2004 The interior transmission problem for anisotropic Maxwell's equations and its applications to the inverse problem *Math. Methods Appl. Sci.* **27** 2111–29

[24] Haddar H and Monk P 2002 The linear sampling method for solving the electromagnetic inverse medium problem *Inverse Problems* **18** 891–906

[25] Kirsch A and Monk P 1995 A finite element/spectral method for approximating the time harmonic Maxwell system in R^3 *SIAM J. Appl. Math.* **55** 1324–44

Kirsch A and Monk P 1998 A finite element/spectral method for approximating the time harmonic Maxwell system in R^3 *SIAM J. Appl. Math.* **58** 2024–8 (corrigendum)

[26] Kress R 2002 Uniqueness in inverse obstacle scattering for electromagnetic waves *Proc. URSI General Assembly Maastricht* (http://www.num.math.uni-goettingen.de/kress/researchlist.html)

[27] Liseno A and Pierri R 2004 Shape reconstruction by the spectral data of the far-field operator: analysis and performances *IEEE Trans. Antennas Propag.* **52** 899–903

[28] Monk P 2003 *Finite Element Methods for Maxwell's Equations* (Oxford: Oxford University Press)

[29] Nédélec J C 2001 *Acoustic and Electromagnetic Equations. Integral Representations for Harmonic Problems* (New York: Springer)